Journal of the Brazilian Society of Mechanical Sciences and Engineering (2023) 45:651
https://doi.org/10.1007/s40430-023-04565-4

TECHNICAL PAPER

Static in bone implants: standard steady-state torque and primary stability in a bioactive kinetic screw

Carlos Aurelio Andreucci[1] · Elza M. M. Fonseca[2] · Renato N. Jorge[1]

Received: 13 July 2023 / Accepted: 4 November 2023 / Published online: 28 November 2023

Abstract
Establishing a standard measurement for drilling and screwing bone implants in different amounts and qualities of bone tissue, in a simple and adequate way to control and predict results, is the gold standard for successful primary stability and better results on long-term osseointegration. So far, the maximum insertion torque (MIT) has been used as the main parameter to achieve success in primary stability and osseointegration, although it has shown conflicting results in the literature for over four decades when predicting standard or minimum values. Basically, the surgeon's experience guides the planning and execution of the surgical procedure, adapted in each case according to his tactile experience, guided by X-ray analysis and the bone and general conditions of the patient. In this work, using a new biomechanical simple machine as a dental implant, a new method will be described mathematically and experimentally, which standardizes the compression and torque in the implant-bone contact, in five different bone densities, during the achievement of mechanical primary stability. The results described the relationship between the MIT, maximum removal torque, and maximum force of static friction between implant-bone and bone-to-bone, achieving a controlled and predictable standard steady-state torque that maintains equilibrium in elastic stress for the primary stability of bone implants, hereby established for an innovative simple machine Bioactive Kinetic Screw.

Keywords Statics · Bone implants · Maximum insertion torque · Maximum removal torque · Standard torque

1 Introduction

Torque (T) is a special kind of force that applies rotational or angular acceleration in an object. If it is not moving it is going to start spinning faster or slower inherent to the force applied. Rotational equilibrium means that there is no torque, no rotational or angular acceleration in an object. Anytime a force goes straight through the center of rotation of an object, there is no torque from that force ($T_{net} = 0$) [1].

Torque equals the force applied times the distance between this force and the center of rotation ($T = Fr$) and its unit Nm.

In bone osteotomies, drilling, and screwing, torque is manually or by motor applied into the bone, controlled by the surgeon tactile experience. Especially for drilling and screwing bone implants, using an electric surgical motor enhance the predictable results for the surgeon by describing torque, speed, and rotational parameters for future improvements in the surgical techniques [2]. Three factors determine the type of work a motor can produce, speed, torque, and horsepower. Speed is defined as how fast the motor performs its work, the typical units of measurement for rotational motor speed are revolutions per minute (rpm). Work is defined as a force applied over a distance, the same definition of torque that produces rotation when a force acts on a radius (r). Horsepower (HP) is defined as the rate at which work is accomplished being another unit of measurement for power and can be translated into Watts (1 HP = 746 Watts), BTUs (1HP = 2545 BTU), Joules (1 HP = 1.055 J), or any unit of power [3].

Technical Editor: João Marciano Laredo dos Reis.

✉ Carlos Aurelio Andreucci
candreucci@hotmail.com

✉ Renato N. Jorge

[1] Mechanical Engineering Department, Faculty of Engineering, University of Porto, Rua Dr. Roberto Frias, 712, 4200-465 Porto, Portugal

[2] Mechanical Engineering Department, School of Engineering, Polytechnic Institute of Porto, R. Dr. António Bernardino de Almeida 431, 4200-072 Porto, Portugal

Manipulating the connection among speed, torque, and horsepower, an understanding of how they are related to surgical motors, increases the precision during bone osteotomies, and offers parameters for controlled results. If torque remains constant, speed and horsepower are proportional. As the speed or rpm increases, HP increases to maintain constant torque. If speed decreases, HP decreases to maintain constant torque [4].

Friction occurs when two materials resist moving against one another like titanium screwed into the bone. The coefficient of static friction depends on the combined effects of material deformation characteristics and surface roughness, both of which originate from the chemical bonding between the atoms of the materials between their surfaces and any adsorbed material. The fractality of surfaces, a parameter that describes the integration of structural and molecular interactions across a range of scales of surface roughness, plays an important role in determining the magnitude of static friction [5]. The amount of friction generated depends primarily on the materials which are in sliding contact, the coefficient of friction (μ) is a dimensionless quantity that describes the ratio of the force of the friction between two bodies and the force of them pressing together. This coefficient can be used to help to determine the amount of force required to move a drill bit, a screw, or a saw in the bone. The amount of force required to slide a load and overcome the maximum static friction (μ_s), and start the kinetic friction, is calculated by multiplying the coefficient of friction (μ) by the weight of the load for horizontal forces, where F_f is the frictional force and N is the normal force (mg), as seen in Eq. (6).

$$F_f = \mu N \tag{1}$$

If an object is on a flat surface and subjected to an external force sliding, then the normal force between the object and the surface is N = mg + Fd only where mg is the object's weight and Fd is the component of the external force (MIT). The coefficient of friction has different values for static friction and kinetic friction. In static friction, the frictional force resists force that is applied to an object, and the object remains at rest, like dental implants totally screwed into the bone, resulting from molecular interactions between the implant and the bone surface. In kinetic friction, the frictional force resists the motion of an object like during the drilling bone. The frictional force itself is directed oppositely to the motion of the object.

How hard the materials are pressed together puts more of their surfaces in contact with each other, and that is where the BKS increased material density plays an advantage [8]. Static friction is required for dental implants primary stability or mechanical stability avoiding micro-movements that lead to increased failure in osseointegration. Maximum insertion torque (MIT) is mistakenly used as a parameter for mechanical initial stability in dental implants clinical and experimental procedures, as observed by conflicting results in literature for decades [9]. Over-tightening the implant into the bone will strip the bone threads, while under-tightening may cause the screws to loosen.

Achieving higher torques in dental implants due to an increased coefficient of friction and not due to undersized drilling compression, increases the bone–implant contact (BIC) surface area without overloading the bone with high stress/strain, as is the case with MIT, mainly due to the difference between the undersized drilling in the bone (smaller diameter) and the geometry of the metal bone implant (screwed under pressure). The different hardness of bone and metal implants increase the stress/strain in the bone, increasing the risk of osseointegration failure [10]. As bone density varies, it is impossible to accurately predict the optimized undersize of the holes for each specific implant geometry. It is used in the literature on different undersized drilling protocols, related to bone densities and implant properties without clear correlation of the results [11]. The higher torque obtained by compression of the implant screw into the bone can cause initial mechanical stability, but it also shows an osteoclastic increase in the early days of the healing process, increasing the risk of implant failure [12]. Once fully screwed into the bone, the dental implant reaches static friction (stability). This is the parameter that prevents micro-movements of the implant in the bone and its value determines the load that can be mechanically supported at this stage of the healing process without compromising short and long-term osseointegration.

If, immediately after obtaining MIT, we apply an anti-torque (MRT) to the same implant, as soon as it begins to move, we obtain exactly the value of torque (force) required to overcome maximum force of static friction, or maximum static friction torque (MSFT) applied to screw removal, equivalent to the maximum removal torque (MRT) in implants, which has already been robustly described in the literature. This is only possible in experimental studies in the laboratory or on animals, otherwise, osseointegration is compromised by loosening the implant [13]. The implant site preparation protocol should be carefully chosen to reduce implant micromovement below the 50-150 μm threshold and to provide adequate stability and prosthetic support according to the planned loading protocol (delayed, early, or immediate) [14]. This implant-bone interface contact (BIC) does not consider the contact volume between these materials. With different drilling parameters and protocols, its unpredictable in humans that the maximum static friction torque (MSFT) or MRT, and different MIT standards are described in the literature as ideal, with differences between 10 and 150 Ncm, showing discrepancies and inconsistencies in the results [15, 16]. There are also

no correlations between different primary stability analysis tests, such as resonance frequency analysis (RFA), implant stability quotient (ISQ), insertion energy (IE) measurements, i.e., the total energy required to place the implant in its site, and implant to bone MIT [17]. In a systematic review, the mean value of micromotion for implants that osseointegrated was 32% of the mean value for those that did not (112 ± 176 µm versus 349 ± 231 µm, $p < 0.001$) [14].

As it is also a drill bit, with BKS there is no lateral compression after total insertion into the bone bed due to the bone being cut by the flutes of the same size and geometry as the BKS implant. The retention and immobilization of the BKS being done primarily by the resulting force (torque) applied through the implant into the bone, correlated with the coefficient of kinetic friction of the implant into the bone (μ_{KIB}) and the coefficient of kinetic friction (μ_{KBB}) of the compacted bone (chips) inside and through the BKS to the bone bed site (μ_{KBB}, or bone to bone kinetic friction) until the torque is removed, becoming the BKS coefficient of static friction ($BKS\mu_{SF}$) [18, 19]. The depth where the torque increases more abruptly has been considered as the point of flute clogging (bone chips) and used as a performance criterion for chip-evacuation capability [20, 21]. In BKS insertion (μ_{KIB}), the increase in torque indicates the start of compaction of the collected material, where the addition of more torque continuously reaches the limit (μ_{KBB}) allowed and established by the properties of the materials used, without breaking the integrity of the system and causing rupture (ultimate strength) [21].

Chips can be classified as granular solids, which are characterized as a group of particles of approximately the same size. Granular solids have characteristics of both fluids and solids. They occupy the internal geometry of the BKS, as shown in Figure 1, where they fill, exert pressure on the container boundaries, and flow through openings like fluids. However, like solids, they have cohesive strength, can have non-isotropic stress distributions, and have shear stresses proportional to normal stress [20].

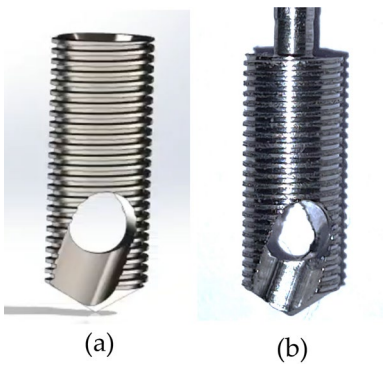

Fig. 1 (a) BKS, innovative biomechanism for bone screws and implants; (b) BKS machined for the experiment in steel 304

Bone drilling chips (bone graft) collected during implant site preparation can be reused as homogenous autologous bone graft material to increase the coefficient of friction values due to cohesive molecular retention of bone particles in the bone bed site [20, 21]. It is well-known in the literature that living cells have been found in bone chips even after drilling with twist drills [22]. The measured value obtained in vitro, and ex vivo experiments determined the torque values for five different synthetic bone densities (polyurethane foam) PCF 10, 15, 20, 30, and 40. The biomechanical results can be mathematically hypothesized for human application by the similar and proportional relationship observed in this and other experimental tests [23] even with different bone densities, using the same protocol [24].

2 Materials and methods

The forces of torque (MIT and MRT), and coefficient of friction analysis, covered by this study, aim to find the required rotational moment to push (insertion) and pull (removal) BKS to impending motion. As impending motion is the threshold between the system holding still and moving, the knowledge of the moments required at impending motion allows you to interpret what happens to the BKS system in static-but-not-impending conditions as well. Since all friction is impending, we will use the maximum coefficient of static friction (μ_{SF}) after reaching the MIT (equal to F_d) and the related friction force (F_f or MRT) to describe the maximum insertion force associated directly to (μ_{SF}) by the Eq. (2), where the normal force (N) equals to weight (mg), applied as follows:

$$\mu_{SF} = \frac{F_f}{N + F_d} = \frac{MRT_{BKS}}{mg + MIT_{BKS}} \tag{2}$$

The innovation presented by the BKS bone implant is that after the implant is fully screwed in (MIT), it achieves static friction without lateral pressure into the bone, due to its drill properties [25–28]. By applying the anti-torque (MRT) to the BKS, as soon as the BKS implant starts to move, we can precisely measure the value of the maximum static friction force limit that will avoid micro-movements of the implant inside the bone to achieve successful primary stability (mechanical stability).

In the experiment to determine the maximum static friction force (F_{SF}), a new standard torque (ST) obtained will be proposed, correlated with success or failure probabilities in osseointegration. Our *ST* proposal is described by the *MIT* relationship with *MRT*, obtaining the amount of force (F_{SF}) to start unscrewing the implant (BKS). This approach is only valid for individual measurements on implants that are inserted without any bone bed compression when the bone

bed size is drilled at the same size as the implant geometry. It is not possible to obtain controlled similar values and predictions using this method, in any protocol of undersized bone drilling, and perforations with unthreaded holes, applied in bone implants. The Eq. (3) to determine the standard torque (*ST*) for BKS is:

$$\mathrm{ST_{BKS}} = \mathrm{MRT_{BKS}} \tag{3}$$

The ST will be a non-absolute value but proportional to the bone densities applied. Higher the MIT then higher the MRT, but due to the properties of BKS the measured difference between MIT and MRT remains proportional and predictable. The Coefficient of Friction (μ) is the measure of the amount of interaction between two surfaces related to the friction between them, as they slide over one another, roll over one another, or two surfaces are in contact but not moving. They are acted upon by forces in opposite directions, and then, since they do not move and there is still an interaction, the amount of interaction depends on the coefficient of friction between them. In maximum static friction when a force (F_{SF}) is applied and eventually the object begins to move this is defined as the static coefficient of friction (μ_{SF}), distinct from the kinetic coefficient of friction. Mathematically it can be represented by an Eq. (4) between the $\mathrm{MRT_{BKS}}$ which is equal to the static friction force (F_{SF}), the force applied at the same distance (the radius of the BKS) making it possible to compare these two forces, required to start moving the implant anticlockwise, divided by the normal force (N) sum with the external force (MIT) of the object as follows equations:

$$\mathrm{MRT_{BKS}} = F_{\mathrm{SF}} \tag{4}$$

$$\mu_{\mathrm{SF}} = \frac{F_{\mathrm{SF}}}{mg + F_d} \tag{5}$$

The force ($\mathrm{MRT_{BKS}}$ or F_{SF}) required to start moving the BKS implant divided by the normal force $N = \mathrm{mg} + \mathrm{Fd}$ only where mg is the object's weight and F_{d} is the component of the external force (MIT), is equal to the maximum static coefficient of friction (μ_{SF}) of the BKS into the bone.

With the experimental results obtaining the $\mathrm{MRT_{BKS}}$ that is equal to F_{SF} we can precisely determine the static coefficient of friction (μ_{SF}) using Eqs. (4), and (5), correlating it in different bone densities. Measuring the $\mathrm{MRT_{BKS}}$ and applying its correlation with a static coefficient of friction (μ_{SF}), we can predict the amount of force (F_{SF}) or standard torque (ST_{BKS}) that the mechanical primary stability will support to avoid micromotions and lead to secondary stability promoting osseointegration as seeing on Eq. (3).

Knowing μ_{SF} and N applying Eq. (5) we can determine F_{SF}. From Eq. (4) we know that F_{SF} is equal to $\mathrm{MRT_{BKS}}$. Without applying $\mathrm{MRT_{BKS}}$ into the implant, the standard torque ($\mathrm{ST_{BKS}}$) proposed can be mathematically determined with precision and safety, without compromising osseointegration, allowing to have improved data collection, precise adjustments on the surgical protocols planning, and controlling the osseointegration predictable results based on mechanical primary stability.

Twenty BKS implants [--] were machined in steel 304 with the size of 10 mm length and 4 mm diameter to be tested in synthetic bones (Nacional Ossos Ltda.) in five distinct densities, PCF 10, 15, 20, 30 and 40. Implants were inserted manually with a surgical electrical motor (Tech Drill) and the torques (MIT and MRT) was measured by TQ 8801 digital torque meter. The MIT and MRT values were considered individually for each implant to achieve accuracy in comparing the results of the coefficient of friction and the amount of compacted bone inside. Visual inspection of the quality of bone compaction during drilling and screw insertion was performed immediately after obtaining the MRT and unscrewing the BKS. After weighing the screw, tweezers were used to remove the compacted material inside, demonstrating the densification effect by removing the bone in a block rather than in grains, as shown in Figure 2.

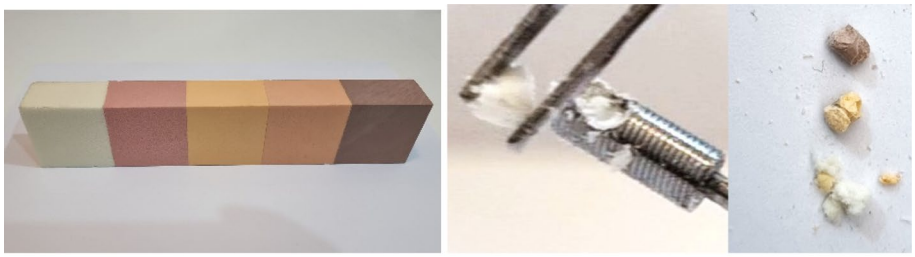

(a) (b)

Fig. 2 (a) Synthetic bones in five distinct densities (PCF 10, PCF 15, PCF 20, PCF 30, and PCF 40); and (b) removal of compacted bone inside the BKS after unscrewing. Using the tweezers, it is possible to visualize the block of bone formed by the innovative properties of compaction of the material inside, rather than the particulate material (grains) that occurs with traditional drilling. Different bone densities in the experiment had the same BKS compaction effect. The compaction ratios were relative to the density of each bone

All BKS implants were weighed before bone insertion and after total removal to accurately measure the amount of bone graft collected using the Brifit precision digital scale, and these values were used individually in the calculations as seen in Figure 3.

3 Results and discussion

A new measure of the volumetric coefficient of friction (μV) when there is full contact between the walls of a volume of material that is inserted into another material, with one of the surfaces being subjected to the insertion force was determined in this work. In all the measurements made, the MRT was always higher than the MIT, which is an innovative property of the BKS used as a dental implant in this work. A pattern was observed when obtaining the torque values. At the beginning of the simultaneous drilling and screwing, a constant torque is obtained, which gradually increases until it reaches the MIT as soon as the material begins to be compacted inside the BKS. It has been observed that the compaction and densification of the material inside the BKS (Fig. 2b) produces the superior locking of the BKS, requiring a higher torque (MRT) for its removal than that used for its insertion (MIT). This innovative feature represents a major advance in the field of implantology, considering the precise control of the values obtained and their standardization to determine the torque and force that immediate connections and prostheses can withstand. In addition, the densification of the bone inside the BKS makes the low-density bones (PCF 10 and PCF 15) inside the BKS similar or superior to the amounts of higher density bones studied here (PCF 20, PCF 30) [8]. Considering the non-uniform biomechanical properties of the bones, obtaining a precise relationship proportional to the MIT obtained and its relationship with μ_{SF} and MRT, we have obtained a new fundamental tool through BKS properties for understanding the relationship of primary stability of bone implants, the contact surface and its relationship with bone quantity and quality.

Ten measurements were taken for each bone density and only the lowest values were used in this study to maintain a direct relationship between individual MIT and MRT values. It was decided not to use the average of the values obtained from all the measurements to accurately determine the values of the coefficient of friction for each bone density studied. The lower values of MIT and MRT determined and applied in this study make it possible to predict the torque and load that the BKS implant will support with a margin of safety to be tested.

The results presented in Table 1 show that in all different bone densities, the determined minimum friction factor was greater than 1. This standardization of the μ_{SF} in the different bone densities is the desired solution for cases where the quantity and the quality of the bone is low.

Knowing that the total volume of bone compacted inside the BKS is 96.91 mm^3 [8], the densification value of the different bone densities (Table 1) was accurately determined. The average compaction value found was 3.45 times higher than the original density of the bones, validating previous studies [8].

The stability parameters measured for dental implants in D1 bones (PCF 40) are all higher than those measured in the D4 bones (PCF 10). In general, a higher insertion speed results in a lower MIT while the insertion stability coefficient (ISQ) differed significantly among the insertion speeds [29]. The increase in MIT reduces the value of micromotions between the implant and bone interface. Some authors indicate immediate loading as a valid therapeutic choice in

(a) (b)

Fig. 3 (a) BKS, innovative biomechanism for bone screws and implants dry weight before insertion into the bones; (b) and BKS filled with synthetic bone after application MRT, showing total weight after removal from bone

Table 1 Obtain μ_{SF} values by applying MIT, and MRT values and determine the amount of bone collected by BKS at the different bone densities studied

	Density (g/cm3)*	MIT (N/cm)	MRT (N/cm)	Collected weight (g)	Total weight (g)	μsf
PCF 10	0.16	20	21	0.059	0.91	1.05
PCF 15	0.24	22	23	0.082	0.933	1.05
PCF 20	0.32	30	32	0.11	0.961	1.07
PCF 30	0.48	44	47	0.165	1.016	1.07
PCF 40	0.64	52	57	0.22	1.071	1.1

low-density D4 trabecular bones with at least 45 N/cm MIT obtained with the use of compression drilling techniques. [30]. Clinical determination of bone density during drilling can be obtained in cortical and trabecular bone but not in intermediate densities. Increasing peak MIT values correlated with increasing bone volume and higher MIT, does not seem to alter the osseointegration process [15, 31].

Histological imaging with those obtained by X-ray absorption images from synchrotron radiation micro-computed tomography, is considered the gold standard for analyzing bone formation around metallic implants. Comparing statistically the results of bone–implant contact (BIC) showed a non-significant difference of 1.9 % ($p = 0.703$), and bone–implant volume (BIV) showed a non-significant difference by only 1.4 % ($p = 0.736$) [32].

The major factors affecting the MIT are bone density and hardness, use or not of under-dimensioned drills, and tapered implant design. The MIT achieved is directly proportional to the bone density, higher in D1 density and lowest in D4 density, without the use of compression techniques. Using under sized drilling techniques it is possible to achieve better stability by compression improving MIT in poor quality bone. Over-compression (high stress) could compromise the angiogenesis and new blood vessel formation [33]. Leading to hypoxia in bone–implant tissues inhibiting bone formation and affecting Secondary biological stability.

The interstitial fluid supplying the bone cells transmits external stresses to bone cells through mechanical energy from external stresses are converted into bioelectric and biochemical signals modulating bone cell metabolism, called mechano-transduction. When these external stresses are too high, osteocytes die, and emerging osteoclasts and bone tissue breakdown affecting osseointegration [34]. MIT is reduced in implant macro-designs that incorporated cutting edges, and lower insertion torque (IT) is associated with decreased micromovement as this thread-cutting geometry creates a high level of bone to implant contact [35]. Findings in the literature suggest that a rough surface finish to cut bone, in a well-reduced fracture, should promote healing by stabilizing the fracture interface [36].

The tribological properties from the friction of the bone, and titanium and its alloys should be considered, both exhibiting friction wear. In the bone, wear is more severe than titanium and its alloys. The wear debris (chips) from the bones should be considered influencing the micromotion by stiffness or looseness of the implants. [37]. The wear form of bone is a plastic deformation with critical digs, debris, and microcracks, whereas while that of the Titanium Alloy (Ti-6Al-4V) is a micro-cutting with scratches, denoting adhesive, and abrasive wear. [38].

Authors [39] validated testing methods to provide bone–implant friction data concluding that the rotation method, like when screwing, presented accurate friction estimates, and was less affected by normal force (N) and speed, than the sled method. The testing of bone against implant surfaces produced a variety of different force displacement curves and a wide range of friction coefficients in bovines, ranging from 0.19 to 0.78. A weak positive correlation was observed between bone porosity and friction coefficient.

A dental implant's macro geometry is critical to its primary stability. Primary stability is improved by increasing the contact surface of the implant with the surrounding bone through a larger diameter, conical shape, and roughened surface. This is considered the basis for successful implant osseointegration, which can be influenced by various factors such as implant design [40, 41]. The undersized drilling technique for implant site preparation results in increased insertion torque in sites with low bone density [42], and the innovative BKS proposal to drill and screw simultaneously shows an improvement in this type of protocol. In previous studies, an analytical-experimental comparison of implant screws of the same size with and without the BKS biomechanism described the achievement of steady state with BKS [43].

The results obtained in the experiments with BKS in the form of a dental implant showed that the presented new biomechanism preserves the bone perforated in the same place inside the BKS, increases the MIT in proportion to the compacted bone inside it, makes the MRT superior in values to the MIT for bone adhesion and cohesion within the BKS in contact with the bone bed. The BKS also made it possible to control and predict the results in the different bone densities used in this study. If the recipient site does not have a flat base for direct insertion of the BKS, a previous guide hole of 1.6 mm in is indicated to ensure correct positioning of the implant, reducing the compacted bone density inside the BKS, but still increasing the density compared to the original bone [8]. If a temporary bone screw is chosen, the limitations of BKS must be considered, given the tendency to increase primary locking and thus optimize osseointegration in the medium and long-term.

4 Conclusions

The new simple machine BKS in the form of a dental implant showed a higher MRT than MIT in all the experiments carried out. In soft bone (PCF 10 and PCF 15) the minimum values obtained were 21 N/cm and 23 N/cm, respectively. In medium hard bone (PCF 20 and PCF 30), the minimum values obtained were 32 N/cm and 47 N/cm, respectively. In hard bone (PCF 40) a minimum value of 57 N/cm was obtained. The coefficient of friction between bone and BKS remained above 1 in all measurements performed. The lowest MRT values obtained at all bone hardness set a

standard for the maximum load that can be safely applied to BKS, where the maximum torque value (MIT) obtained as a standard in dental implant surgery, which is always lower than the MRT in all measurements, it indicates, without the need to apply the MRT, how much is the maximum force that can be applied for tighten and loosen abutment screws and temporary teeth. The value of MIT will vary with the hardness of the bone but will always present a higher MRT for its removal, making the value of MIT obtain a safe range of load that the bone implant can support. Using average values to determine MIT and MRT should be avoided in experimental studies. This work showed the importance of directly comparing MIT and MRT values in the same bone implant to obtain the true values of the coefficient of friction. This is only possible with the new technique used at BKS, where the insertion of the dental implant is standardized by its experimentally determined properties and characteristics. Future work with in vivo studies will determine whether this ratio of MRT greater than MIT is maintained in the organic environment.

Acknowledgements Not applicable.

Author's contribution Conceptualization contributed by CAA; methodology contributed by CAA; formal analysis contributed by CAA; investigation contributed by CAA; writing—original draft preparation contributed by CAA; writing—review and editing contributed by EMMF; visualization contributed by EMMF; supervision contributed by RNJ. All authors have read and agreed to the published version of the manuscript.

Funding Open access funding provided by FCT|FCCN (b-on).

Data availability statement Not applicable.

Declarations

Conflicts of interest The authors have no relevant financial or non-financial interests to disclose.

References

1. Hansen EA, Smith G (2009) Factors affecting cadence choice during submaximal cycling and cadence influence on performance. Int J Sports Physiol Perform 4(1):3–17. https://doi.org/10.1123/ijspp.4.1
2. Kandavalli SR, Wang Q, Ebrahimi M, Gode C, Djavanroodi F, Attarilar S, Liu S (2021) A Brief review on the evolution of metallic dental implants: history, design, and application. Front Mater 8:646383. https://doi.org/10.3389/fmats.2021.646383
3. Lee D-H, Cho S-A, Lee C-H, Lee K-B (2015) The Overuse of the Implant Motor. Clin Implant Dent Relat Res 17:435–441. https://doi.org/10.1111/cid.12195
4. Neugebauer J, Scheer M, Mischkowski RA et al (2009) Comparison of torque measurements and clinical handling of various surgical motors. Int J Oral Maxillofac Implants 24:469–476
5. Hanaor DAH, Gan Y, Einav I (2016) Static friction at fractal interfaces. Tribol Int 93:229–238. https://doi.org/10.1016/j.triboint.2015.09.016
6. Castagnetti D, Dragoni E (2012) Predicting the macroscopic shear strength of adhesively-bonded friction interfaces by microscale finite element simulations. Comput Mater Sci 64:146–150
7. Gnecco E, Bennewitz R, Pfeiffer O, Socoliuc A, Meyer E (2011) Friction and wear on the atomic scale. Springer, Nanotribology and Nanomechanics II, pp 243–292
8. Andreucci CA, Fonseca EMM, Jorge RN (2022) Increased material density within a new biomechanism. Math Comput Appl 27:90. https://doi.org/10.3390/mca27060090
9. Wilkie J, Rauter G, Möller K (2022) Determining relationship between bone screw insertion torque and insertion speed: Bestimmung des Zusammenhangs zwischen dem Drehmoment beim Eindrehen von Knochenschrauben und der Eindrehgeschwindigkeit. at—Automatisierungstechnik. 70(11):976–991. https://doi.org/10.1515/auto-2022-0009.
10. Kochar SP, Reche A, Paul P (2022) The etiology and management of dental implant failure: a review. Cureus 14(10):e30455. https://doi.org/10.7759/cureus.30455
11. Jimbo R, Tovar N, Anchieta RB et al (2014) The combined effects of undersized drilling and implant macrogeometry on bone healing around dental implants: an experimental study. Int J Oral Maxillofac Surg 43(10):1269–1275. https://doi.org/10.1016/j.ijom.2014.03.017
12. Berardini M, Trisi P, Sinjari B, Rutjes AWS, Caputi S (2016) The effects of high insertion torque versus low insertion torque on marginal bone resorption and implant failure rates: a systematic review with meta-analyses. Implant Dent 25(4):532–540. https://doi.org/10.1097/ID.0000000000000422
13. Comuzzi L, Tumedei M, Romasco T et al (2022) Insertion torque, removal torque, and resonance frequency analysis values of ultrashort, short, and standard dental implants: an in vitro study on polyurethane foam sheets. J Funct Biomater 14(1):10. https://doi.org/10.3390/jfb14010010
14. Kohli N, Stoddart JC, van Arkel RJ (2021) The limit of tolerable micromotion for implant osseointegration: a systematic review. Sci Rep 11:10797. https://doi.org/10.1038/s41598-021-90142-5
15. Makary C, Rebaudi A, Mokbel N, Naaman N (2011) Peak insertion torque correlated to histologically and clinically evaluated bone density. Implant Dent 20(3):182–191. https://doi.org/10.1097/ID.0b013e31821662b9
16. Stocchero M, Jinno Y, Toia M et al (2023) Effect of drilling preparation on immediately loaded implants: an in vivo study in sheep. Int J Oral Maxillofac Implants 38(3):607–618. https://doi.org/10.11607/jomi.9949
17. Raz P, Meir H, Levartovsky S, Sebaoun A, Beitlitum I (2022) Primary implant stability analysis of different dental implant connections and designs-an in vitro comparative study. Materials 15(9):3072. https://doi.org/10.3390/ma15093072
18. Bulaqi HA, Mousavi Mashhadi M, Geramipanah F, Safari H, Paknejad M (2015) Effect of the coefficient of friction and tightening speed on the preload induced at the dental implant complex

with the finite element method. J Prosthet Dent 113(5):405–411. https://doi.org/10.1016/j.prosdent.2014.09.021
19. Hao CP, Cao NJ, Zhu YH et al (2021) The osseointegration and stability of dental implants with different surface treatments in animal models: a network meta-analysis. Sci Rep 11:13849. https://doi.org/10.1038/s41598-021-93307-4
20. Mellinger JC, Burak Ozdoganlar O, DeVor RE, Kapoor SG (2002) Modeling chip-evacuation forces and prediction of chip-clogging in drilling. ASME J Manuf Sci Eng 124(3):605–614. https://doi.org/10.1115/1.1473146
21. Andreucci CA, Fonseca EMM, Jorge RN (2023) A New Simplified Autogenous Sinus Lift Technique. Bioengineering 10:505. https://doi.org/10.3390/bioengineering10050505
22. Babczyk P, Winter M, Kleinfeld C, Pansky A, Oligschleger C, Tobiasch E (2022) Examination of the quality of particulate and filtered mandibular bone chips for oral implants: an in vitro study. Appl Sci 12:2031. https://doi.org/10.3390/app12042031
23. Andersen OZ, Bellón B, Lamkaouchi M et al (2023) Determining primary stability for adhesively stabilized dental implants. Clin Oral Invest. https://doi.org/10.1007/s00784-023-04990-8
24. Kamel S, Mohamed N, Sherif M, Hee-Moon K, El-K A (2017) In vitro assessment of maximum insertion and removal torque with three different miniscrews on artificial maxilla and mandible. J World Fed Orthodon 6(3):115–119. https://doi.org/10.1016/j.ejwf.2017.08.003
25. Andreucci CA, Alshaya A, Fonseca EMM, Jorge RN (2022) Proposal for a new bioactive kinetic screw in an implant. Using Numer Model Appl Sci 12:779. https://doi.org/10.3390/app12020779
26. Andreucci CA, Fonseca EMM, Jorge RN (2022) 3D printing as an efficient way to prototype and develop dental implants. BioMedInformatics 2(4):671–679. https://doi.org/10.3390/biomedinformatics2040044
27. Andreucci CA, Fonseca EMM, Natal RMJ (2022) Structural analysis of the new Bioactive Kinetic Screw in titanium alloy vs. commercially pure titanium. J Comp Art In Mec Biomecd 2:35–43. https://zenodo.org/badge/DOI/10.5281/zenodo.7406075.svg
28. Andreucci CA, Fonseca EMM, Jorge RN (2023) Bio-lubricant properties analysis of drilling an innovative design of bioactive kinetic screw into bone. Designs 7(1):21. https://doi.org/10.3390/designs7010021
29. Hsu YY, Tsai MT, Huang HL et al (2022) Insertion speed affects the initial stability of dental implants. J Med Biol Eng 42:516–525. https://doi.org/10.1007/s40846-022-00742-3
30. Trisi P, Berardi D, Paolantonio M, Spoto G, D'Addona A, Perfetti G (2013) Primary stability, insertion torque, and bone density of conical implants with internal hexagon: Is there a relationship? J Craniofac Surg 24(3):841–844. https://doi.org/10.1097/SCS.0b013e31827c9e01
31. Andreucci CA, Fonseca EMM, Jorge RN (2023) Immediate autogenous bone transplantation using a novel kinetic bioactive screw 3D design as a dental implant. BioMedInformatics 3(2):299–305. https://doi.org/10.3390/biomedinformatics3020020
32. Bernhardt R, Kuhlisch E, Schulz MC, Eckelt U, Stadlinger B (2012) Comparison of bone-implant contact and bone-implant volume between 2D-histological sections and 3D-SRμCT slices. Eur Cell Mater 23:237–248. https://doi.org/10.22203/ecm.v023a18
33. Checa S, Prendergast PJ (2010) Effect of cell seeding and mechanical loading on vascularization and tissue formation inside a scaffold a mechano-biological model using a lattice approach to simulate cell activity. J Biomech. 43(5):961e968
34. Burger EH, Klein-Nulend J (1999) Mechanotransduction in bonedrole of the lacuno-canalicular network. FASEB J. (13):S101eS112
35. Freitas Jr AC, Bonfante EA, Giro G, Janal MN, Coelho PG (2012) The effect of implant design on insertion torque and immediate micromotion. Clin Oral Impl Res. 23:113e118. https://doi.org/10.1111/j.1600-0501.2010.02142.x.
36. Shockey JS, von Fraunhofer JA, Seligson D (1985) A measurement of the coefficient of static friction of human long bones. Surf Technol 25(2):167–173. https://doi.org/10.1016/0376-4583(85)90030-5
37. Bihai Z, Xiaofeng H, Tianliang Z (2015) Friction and wear characteristics of natural bovine bone lubricated with water, Wear. 322–323. https://doi.org/10.1016/j.wear.2014.10.013
38. Chenchen W, Gangqiang Z, Zhipeng L, Ze X, Yong X, Shichang Z, Hongxing H, Yadong Z, Tianhui R (2019) Tribological behavior of Ti-6Al-4V against cortical bone in different biolubricants. J Mech Behav Biomed Mater 90:460–471. https://doi.org/10.1016/j.jmbbm.2018.10.031
39. Dannaway J, Dabirrahmani D, et al. (2015) An investigation into the frictional properties between bone and various orthopedic implant surfaces—implant stability. J Musculoskelet 18. https://doi.org/10.1142/S0218957715500153
40. Heimes D, Becker P, Pabst A et al (2023) How does dental implant macrogeometry affect primary implant stability? A narrative review. Int J Implant Dent 9:20. https://doi.org/10.1186/s40729-023-00485-z
41. Lemos CAA, Verri FR, de Oliveira Neto OB et al (2021) Clinical effect of the high insertion torque on dental implants: a systematic review and meta-analysis. J Prosthet Dent 126(4):490–496. https://doi.org/10.1016/j.prosdent.2020.06.012
42. Heinemann F, Hasan I, Bourauel C, Biffar R, Mundt T (2015) Bone stability around dental implants: treatment related factors. Ann Anat 199:3–8. https://doi.org/10.1016/j.aanat.2015.02.004
43. Andreucci CA, Fonseca EMM, Jorge RN (2023) A new simple machine that converts torque into steady-state pressure in solids. In: 2023 IEEE 7th Portuguese meeting on bioengineering (ENBENG), Porto, Portugal, pp 148-150. https://doi.org/10.1109/ENBENG58165.2023.10175336